American Mineralogist, Volume 74, pages 642–655, 1989

Kornerupine: Chemical crystallography, comparative crystallography, and its cation relation to olivine and to Ni_2In intermetallic

Paul Brian Moore
Department of Geophysical Sciences, The University of Chicago, Chicago, Illinois 60637, U.S.A.
Pradip K. Sen Gupta
Department of Geology, Memphis State University, Memphis, Tennessee 38152, U.S.A.
Elmer O. Schlemper
Department of Chemistry, University of Missouri, Columbia, Missouri 65211, U.S.A.

Abstract

Kornerupine from Mautia Hill, Tanzania, orthorhombic holosymmetric, $a = 16.041(3)$, $b = 13.746(2)$, $c = 6.715(2)$ Å, space group *Cmcm*, $Z = 4$, formula from refined structure $Mg_{3.98}Fe^{3+}_{0.38}Al_{5.47}Si_{4.11}B_{0.43}O_{21.24}(OH)_{0.76}$, has been refined to $R = 0.027$ for 1807 independent reflections.

One partly occupied site [X] with distorted cubic coordination by oxygen, five octahedral sites [M(1)–M(5)], three tetrahedral sites [T(1)–T(3)], and ten oxygen atoms [O(1)–O(10)] occur in the asymmetric unit of structure. Several earlier suggestions were verified: the X site population is partly occupied and refined to 0.374Mg + 0.626□; all B is sequestered at T(3) = 0.572Si + 0.428B, and the distorted M(4) site sequesters reported Fe^{3+}, 0.810Al + 0.190Fe^{3+}. In addition, anisotropic thermal-vibration parameters U_{ii} have average differences of 25% between pairs of 18 fully occupied sites in this structure and in two earlier well-refined structures. O(10) is bonded in part to a H atom that is believed to form a hydrogen bond O–H(10)···O(9) with an O(10)–O(9) length of 2.763 Å, a reasonable coupled relation to X being $X^{2+}_{1/3}\square_{1/3}(OH)^{-}_{2/3}$.

By analogy with $[P_4] \rightarrow [P_4O_6] \rightarrow [P_4O_{10}]$, it is believed that generalized kornerupine, $M_{40}T_{20}O_{88}$, which has a cation pseudorepeat of $a/5$ or $M_8T_4O_{17.6}$, is a dilated version of the intermetallic Ni_2In, as is also asserted for the olivine structure type. The model based on *s-s*, *s-p*, and *p-p* bond strengths suggested by Pauling and the $[P_4] \rightarrow [P_4O_6] \rightarrow [P_4O_{10}]$ structure sequence appear to explain not only the relation to Ni_2In but also the location of oxygen sites in that structure type, of which many alternative anion loci are structurally possible. Thus, kornerupine and sinhalite (olivine), which occur in similar parageneses, are different ways of stuffing interstitial oxygen between cations of similar arrangement.

Introduction

Contemporary crystal-structure analysis is rarely an end in itself. Beyond solution and characterization of novel structure types, comparative relations are often sought within a composition series. Usually the quality of a refinement hinges on the quality of the crystal. Most important parameters include the linear atomic-absorption coefficient, μ, the anisotropic thermal-vibration ellipsoids for the independent atomic sites, the site population for each of these independent sites, mosaicity, secondary extinction, and the refined atomic coordinates themselves. Even if all of these conditions are known to perfection, a perfect refinement still cannot exist because of uncertainties inherent in the selected scattering factors and the choice of fully ionized or neutral atoms. The data set is limited by the X-radiation brought upon the crystal. The conventional test of the quality of the data set and all the attendant parameters to be varied is R, the "R factor," "reliability index," "discrepancy index," "residual," etc. In contemporary refinements, R usually ranges from 0.04 to 0.06, and exceptional cases will provide $R = 0.015$–0.04. $R = 0.00$ is clearly impossible, as a perfect X-ray diffraction experiment cannot exist with the limiting criteria outlined above. What about $R > 0.06$? There are many experiments that fall in this region, and when they are reported, a good explanation for this high value is expected from the investigator(s). Typical examples are found in crystals with large μ (say >300 cm^{-1}) and those having cations with associated lone electron pairs and consequent difficulty of crystal measurement in preparation for absorption correction. The other examples are found in crystals that are composed not of one singlet but of two or more individuals each with a different but related structure. Yet others display severe lineage or twinning, but these can be easily tested. These are very com-

0003–004X/89/0506–0642$02.00

mon phenomena, and such structure solutions usually are called "averaged structures."

Kornerupine poses many such hurdles. With 19 independent atoms in the asymmetric unit, 9 of these are cations; most of the cation sites in turn involve solid solution of two or more ionic species, and one site is only partially occupied. At least six chemical components occur for natural kornerupine. In its favor, however, is hardness (7 on Mohs scale) and low linear absorption coefficient, $\mu \approx 14.3$ cm^{-1} (Mo$K\alpha$). Experience suggests that substances of superior hardness usually afford superior diffracta and superior subsequent refinement especially of the anisotropic thermal-vibration parameters, all probably a result of rather uniform distribution of chemical bonds with relatively high bond strength. We would immediately anticipate relatively low average root-mean-square thermal-vibration amplitudes in such cases.

Three previous kornerupine structure studies were reported. The first, by Moore and Bennett (1968), revealed the broad features of the structure and resulted in $R = 0.11$ for 1047 independent data. An end-member composition was proposed: $Mg_3Al_6O_4(OH)[Si_2O_7][(Al,Si)_2SiO_{10}]$. Four formula units made up the structure cell with $a = 16.100$, $b = 13.767$, $c = 6.735$ Å, space group *Cmcm*. This material was from Mautia Hill, Tanzania, the locality that formed the basis of McKie's (1965) detailed chemical and cell results on the species. The excellent crystals from that locality were precisely those used toward the results in our present investigation. It wasn't that the earlier work of Moore and Bennett was *wrong* (the R index was a perfectly adequate "state of the art" result over 20 years ago), but it was *wanting* in certain respects especially for those investigators interested in B metasomatism in minerals of granulite facies. In this case, no recovery of one large, partly occupied site and the disregard of B partitioning in the crystal structure were shortcomings. The second study, by Moore and Araki (1979), defined the partly occupied site and the preferential sequestering of B at one tetrahedral site. The crystal, a synthetic B-rich kornerupine, gave $R = 0.052$ for 1441 independent reflections, with formula-unit composition $Mg_{3.93}Al_{5.90}Si_{3.92}B_{0.57}O_{20.95}(OH)_{1.05}$, $a = 16.016$, $b = 13.758$, $c = 6.720$ Å, space group *Cmcm*. A third investigation, by Finger and Hazen (1980), yielded $R = 0.058$. These results were of sufficiently precise quality (M–O, T–O $\approx \pm 0.003$ Å) that we considered it possible to probe the general kornerupine structure type further through comparison of site partitioning, anisotropic thermal-vibration parameters, and atomic coordinates with a superior refinement of the Mautia Hill kornerupine.

The results are most gratifying. It is shown that comparison of the thermal-vibration parameters between synthetic and natural crystals presents adequate concord and that minor components are well partitioned with $B^{3+} \rightarrow$ T(3) and $Fe^{3+} \rightarrow$ M(4), confirming the provisional conclusions announced in the Moore-Araki study. Finally, $R = 0.027$ for 1807 independent reflections, a good value for such a complex structure.

Table 1. Experimental details for Mautia Hill kornerupine

(A) Crystal cell data	
a (Å)	16.041(3)
b (Å)	13.746(2)
c (Å)	6.715(2)
V (Å^3)	1480.6(1)
Space group	*Cmcm*
Z	4
Formula (a) McKie 1965	$Na_{0.01}Mg_{3.69}Ti_{0.02}Fe^{3+}_{0.37}Al_{6.36}Si_{3.71}B_{0.41}O_{21.75}(OH)_{0.23}$
(b) from structure	$Mg_{3.98}Fe^{3+}_{0.38}Al_{6.47}Si_{4.11}B_{0.43}O_{21.24}(OH)_{0.76}$
ρ_{calc} (g·cm^{-3}) (a)	3.337
(b)	3.288
Specific gravity (McKie, 1965)	3.297
μ (cm^{-1}) (b)	14.3
(B) Intensity measurements	
Crystal size (μm)	140 × 160 × 300
Diffractometer	Enraf-Nonius CAD-4
Monochromator	Graphite
Radiation	Mo$K\alpha$
Scan type	θ–2θ
2θ range	0.5–75°
Scan width	$A = 0.70$, $B = 0.35$, where $\Delta\theta = (A + B \tan\theta)$
Variable horizontal width (w)	where $A = 4.0$, $w = A + \tan\theta$
Maximum scan time (s)	90
Orientation monitors	three orientation standards checked every 200 reflections; 25 reflections used for cell dimensions
Intensity monitors	every 7200 s of X-ray exposure (decay <1%)
Independent reflections	1807, above 2σ, used in refinement
(C) Refinement of the structure	
R	0.027
R_w	0.049

Kornerupine: Experimental details

Pale pink crystals of kornerupine from Mautia Hill, supplied by D. McKie over 20 years ago toward the original structure study, provided the same batch from which our clear crystal was selected. The data reported here are considered superior in every respect to the initial structure study of Moore and Bennett (1968). An outline of the experimental procedure is given in Table 1. Twenty-five high-angle reflections defined the orientation matrix that provided the crystal cell data. The cell edges are each about 0.3% smaller than those reported by McKie, who used back-reflection photographs, Si internal standard, and Cu$K\alpha$ radiation. The data from our prismatic crystal were corrected for absorption anisotropy by ψ scan, a minimal correction owing to the low linear atomic-absorption coefficient of $\mu = 14.3$ cm^{-1} for Mo$K\alpha$ radiation.

The 1807 independent F_o values were put toward structure refinement, beginning with the proposed atom coordinates of Moore and Araki (1979) for a synthetic crystal. Neutral-atom scattering factors and real and imaginary dispersion corrections were taken from Ibers and Hamilton (1974). Refinement minimized $\Sigma\, w(|F_o| - |F_c|)^2$ where w^{-1} = unit weight. The conventional R index mentioned throughout this paper is $R = \Sigma||F_o| - |F_c||/\Sigma|F_o|$. Refinement employed the full-matrix procedure of least-squares with the program SHELX76. Throughout this study, there was no need to challenge centrosymmetric

TABLE 2. Kornerupine: Atomic coordinate parameters

Atom	A*	M	x	y	z	Δ (Å)
X	a	4	0	0	0	
Ni(1)		4	0	0	0	0.00
M(1)	Mg	8	0.12176(5)	0.14031(5)	1/4	
Ni(2)		8	1/10	1/6	1/4	0.50
M(2)	Mg	4	1/2	0.14563(7)	1/4	
Ni(2)		4	5/10	1/6	1/4	0.29
M(3)	Al	8	0.21536(4)	0	0	
Ni(1)		8	2/10	0	0	0.25
M(4)	b	8	0.31366(3)	0.14182(4)	1/4	
Ni(2)		8	3/10	1/6	1/4	0.41
M(5)	Al	8	0.40756(4)	0	0	
Ni(1)		8	4/10	0	0	0.12
T(1)	Si	8	0.40202(3)	0.35299(4)	1/4	
In		8	4/10	1/3	1/4	0.27
T(2)	c	8	0.17842(4)	0.33375(4)	1/4	
In		8	2/10	1/3	1/4	0.35
T(3)	d	4	0	0.34253(8)	1/4	
In		4	0	1/3	1/4	0.13
Mean						0.26
O(1)		8	0.2240(1)	0.0448(1)	1/4	
O(2)		8	0.40367(8)	0.0460(1)	1/4	
O(3)		8	0.40283(9)	0.2355(1)	1/4	
O(4)		16	0.13818(6)	0.09959(7)	−0.0515(2)	
O(5)		8	0.2338(1)	0.2358(1)	1/4	
O(6)		16	0.31671(6)	0.09479(7)	−0.0471(2)	
O(7)		8	0.0824(1)	0.2821(1)	1/4	
O(8)		8	1/2	0.0885(1)	−0.0541(2)	
O(9)		4	0	0.1128(2)	−1/4	
O(10)		4	0	0.0882(2)	1/4	
			Olivine			
M(1)	Mg	4	0	0	0	
Ni(1)		4	0	0	0	0.00
M(2)	Mg	4	0.4897	0.2226	3/4	
Ni(2)		4	1/2	1/6	3/4	0.57
T	Si	4	−0.0731	0.4057	3/4	
In		4	0	1/3	3/4	0.82
Mean						0.46

Note: Cations of kornerupine and olivine compared with Ni_2In. A = scattering factor, M = equipoint rank. Standard errors in parentheses refer to the last digit.

* (a) Site population refined to 0.374(4)Mg + 0.626□. (b) Site population refined to 0.810(4)Al + 0.190Fe. (c) Site population refined to 0.766(5)Si + 0.234Al. (d) Site population refined to 0.572(1)Si + 0.428B.

Cmcm. Finally, secondary extinction correction (Zachariasen, 1968) was applied for this hard crystal, which yielded a small correction, the maximum being 2.6% of $|F_o|$ for the (0 2 2) reflection.

At one point, we concluded that the structure had been fully refined at $R = 0.034$ and proceeded to draft up this communication. However, it became very clear that one atom was misbehaving, namely M(4) with $B_{eq} = 0.12$ Å^2. This unreasonably low value was at least three times smaller than any other value in the asymmetric unit. Since we applied the neutral scattering factors for atoms as listed in Table 2 and used Al for M(4), we were forced to conclude that a heavier atom was preferentially sequestered at this site, and we placed all Fe^{3+} reported by Scoon in McKie (1965) here.

Atomic coordinates for all 19 asymmetric atoms in kornerupine are given in Table 2, and the cations are compared with the perfect model for Ni_2In. A similar comparison is appended for olivine cations, and this becomes a "working table" later on. The values are from Birle et al. (1968) for forsterite. The anisotropic thermal-vibration parameters and equivalent isotropic thermal vibrations appear in Table 3. This table is also discussed in some detail (see below). Bond distances and angles are offered in Table 4. These values are within M–O, T–O ≈ 0.03 Å and T(3)–O(7) ≈ 0.05 Å of the earlier Mautia Hill study. Table 5[1] lists the observed and calculated structure factors of the present study.

KORNERUPINE: CHEMICAL CRYSTALLOGRAPHY

Since kornerupine's essential details have been covered in the earlier work, only the salient features will be cursorily presented. With three superior refinements, some comparative crystallography is in order.

Formula. Two formulae can be offered for Mautia Hill kornerupine, the first based on the analysis of Scoon in McKie (1965), the second computed from the refined crystal structure. Individual site populations were estimated in three ways: fractional site occupancy, as for X, by varying the site-population parameter; use of more than one scattering curve in a complementary fashion, as for M(4), T(2), and T(3); and later calculation based on average M–O, T–O bond distances, assuming a linear relationship among $^{[6]}Mg$–$^{[4]}O$ (2.10 Å), $^{[6]}Fe^{3+}$–$^{[4]}O$ (2.02 Å), $^{[6]}Al$–$^{[4]}O$ (1.91 Å), $^{[4]}Al$–$^{[4]}O$ (1.77 Å), and $^{[4]}Si$–$^{[4]}O$ (1.64 Å) from the tables of effective ionic radii (based on $^{[6]}O^{2-}$ $r = 1.40$ Å) of Shannon and Prewitt (1969). The final assignments are $X = Mg_{0.37}\square_{0.63}$, $M(1) = Mg_{1.00}$, $M(2) = Mg_{0.95}Al_{0.05}$, $M(3) = Mg_{0.08}Al_{0.92}$, $M(4) = Mg_{0.25}Fe^{3+}_{0.19}Al_{0.56}$, $M(5) = Al_{1.00}$, $T(1) = Si_{1.00}$, $T(2) = Al_{0.23}Si_{0.77}$, and $T(3) = B_{0.43}Si_{0.57}$. All atoms for $Z = 4$ were added up, total oxygens fixed at 22, and the charge imbalance was compensated by substituting appropriate OH^- for O^{2-}. The formulae are

$$Na_{0.01}Mg_{3.69}Ti_{0.02}Fe^{3+}_{0.37}Al_{6.36}Si_{3.71}B_{0.41}O_{21.75}(OH)_{0.23} \quad (a)$$

$$Mg_{3.98}\quad Fe^{3+}_{0.38}Al_{5.47}Si_{4.11}B_{0.43}O_{21.24}(OH)_{0.76}, \quad (b)$$

where (a) is from McKie (1965) and (b) is from this study. Densities were calculated for these two formulae and are listed in Table 1. They are within 1.5% of each other, and within 1% of the measured value. Site-population refinements for Fe^{3+} and B are in good accord with the chemical analysis of Scoon. Our Mg and Si totals are high and our Al total is low, but site assignments based on average bond distances are only approximate, as variations occur among structure types. As a point of fact, we have observed similar relations for other structures and conclude that more structure study on Mg-Al-Si solutions is in order.

This study confirms two conclusions announced in the study of Moore and Araki (1979) on synthetic B-rich kor-

[1] A copy of Table 5 may be ordered as Document AM-89-404 from the Business Office, Mineralogical Society of America, 1625 I Street, N.W., Suite 414, Washington, D.C. 20006, U.S.A. Please remit $5.00 in advance for the microfiche.

TABLE 3. Kornerupine: Anisotropic thermal-vibration parameters ($\times 10^3$)

Atom	U_{11}	U_{22}	U_{33}	U_{12}	U_{13}	U_{23}	B_{eq} (Å^2)
X	64.1(31)	16.2(14)	13.8(16)	0	0	−0.2(13)	2.48(10)
M(1)	11.9(3)	8.6(3)	6.6(3)	2.2(2)	0	0	0.71(2)
M(2)	3.9(4)	4.5(5)	11.0(4)	0	0	0	0.51(2)
M(3)	7.0(3)	6.1(2)	2.5(2)	0	0	−0.7(2)	0.41(1)
M(4)	7.6(3)	7.7(2)	9.4(2)	−0.3(1)	0	0	0.65(1)
M(5)	5.9(3)	5.6(2)	3.4(3)	0	0	−0.6(2)	0.39(1)
T(1)	4.2(3)	5.2(2)	4.0(2)	1.0(1)	0	0	0.35(1)
T(2)	16.0(4)	5.6(2)	3.5(2)	−1.6(2)	0	0	0.66(1)
T(3)	3.6(4)	6.7(4)	3.2(4)	0	0	0	0.36(2)
O(1)	8.3(5)	6.9(5)	3.3(5)	0.3(4)	0	0	0.49(3)
O(2)	7.2(5)	6.2(6)	3.5(5)	−0.8(3)	0	0	0.44(3)
O(3)	8.9(5)	6.1(5)	11.1(6)	1.7(4)	0	0	0.69(2)
O(4)	10.6(4)	9.7(4)	4.2(4)	4.1(3)	−1.5(3)	0.5(3)	0.64(2)
O(5)	21.9(8)	13.5(7)	10.3(7)	−0.1(6)	0	0	1.20(3)
O(6)	7.2(4)	8.4(4)	7.2(4)	0.7(3)	−0.4(3)	−0.0(3)	0.60(2)
O(7)	14.6(6)	15.8(7)	8.5(6)	−8.6(6)	0	0	1.02(3)
O(8)	5.3(5)	5.8(5)	9.6(5)	0	0	0.6(1)	0.54(2)
O(9)	4.8(8)	12.8(9)	22.6(11)	0	0	0	1.06(4)
O(10)	8.3(8)	13.1(6)	17.7(11)	0	0	0	1.03(4)

Note: The U_{ij} are coefficients in the expression $\exp[-(U_{11}h^2 + U_{22}k^2 + U_{33}l^2 + 2U_{12}hk + 2U_{13}hl + 2U_{23}kl)]$. The equivalent isotropic thermal parameter is $B_{eq} = (8/3)\pi^2(U_{11} + U_{22} + U_{33})$.

nerupine, that B^{3+} is sequestered in the T(3) site and that Fe^{3+} goes into the M(4) site. In addition, comparison with Finger and Hazen (1980) shows other substitutions by Fe are possible.

Thermal vibration. Isotropic and anisotropic thermal-vibration effects are difficult to appraise, even in contemporary structural refinements. Rather high correlations among variable parameters such as atomic coordinates with at least one degree of freedom, the linear atomic-absorption coefficient, the anisotropy of the crystal shape, and crystal mosaicity—all are coupled to some degree to the at most six independent anisotropic thermal-vibration parameters. Minerals, which often have a large μ compared with organic crystals, are particularly problematic. For this reason, it is common practice to accept anisotropic thermal-vibration parameters in mineral structures as "sponges" that absorb the errors arising earlier among the other variable parameters, particularly those arising from crystal size and crystal shape and from the linear atomic-absorption coefficient.

For reasonably well-refined structures of a complex mineral, it is desirable to compare the thermal-vibration parameters among refined structures. Three such studies have been selected: this study, the earlier Moore and Araki (1979) investigation, and the results of Finger and Hazen (1980). Although Finger and Hazen reported crystal data for a high-Fe kornerupine from Rangeley quadrangle in Maine including average electron-microprobe composition, atomic coordinates and equivalent isotropic thermal parameters B_{eq}, cation occupancies, and polyhedral mean bond lengths, we were anxious to obtain their original refined U_{ij} set. We thank L. W. Finger for providing these data. We note a small (±10%) difference between our computed B_{eq} from U_{ii} (i = 1 to 3) of this output and the result reported in Finger and Hazen. But of more concern is their statement on p. 373, "Moore and Araki also assumed that there was no iron in M(4), an assumption not consistent with the present refinement." The Moore and Araki sample was a synthetic crystal in the system MgO-Al_2O_3-B_2O_3-SiO_2-H_2O, but a variety of other analyses for natural kornerupine was discussed in that paper. Actually, Moore and Araki (p. 335) declared, "Finally, it is quite likely that Fe^{2+} reported in chemical analyses occurs in 4-coordination at the X-position with Fe^{3+} dissolved in the M(4) position. These two distorted sites seem to account for the pleochroism observed for iron-containing kornerupines." In this study, only the crystals of Finger and Hazen and our present one from Mautia Hill contain substantial Fe. It is desirable to outline the partitioning of "heavy" Fe among the sites on the basis of refined fractional occupancies: M(1), 0.36Fe; M(2), 0.30Fe; M(4), 0.12Fe; and X, 0.07Fe according to Finger and Hazen or M(4), 0.19Fe according to this study.

McKie (1965) reported Fe_2O_3 3.98% and FeO *nil* for the Mautia Hill material used in this study. Since the largest sites are X, M(1), and M(2), Fe^{2+} is believed to enter into these, with Fe^{3+} partitioning into the much smaller and also more distorted M(4) site; that is X, M(1), M(2) ≈ (Mg^{2+},Fe^{2+}), and M(4) ≈ (Al^{3+},Fe^{3+}). It would appear that the conditions of formation for the Finger and Hazen (1980) kornerupine were those of relatively lower oxygen fugacity than those for formation of the Mautia Hill material.

Comparison of individual U_{ii} (i = 1 to 3) and of B_{eq} was performed in the following manner. It was asked whether individual values from Moore and Araki (1979) and Finger and Hazen (1980) were relatively greater or less than those from this study, which was used as the reference. We should suspect some significant departures owing to different procedures of data collection and reduction and to deduced site partitionings. As X is only a partly occupied site, it was excluded from comparison. The values for M(1)–M(5), T(1)–T(3), and O(1)–O(10) were calculated as *difference*, Δ, expressed in percent. Setting W to equal

TABLE 4. Kornerupine: Polyhedral interatomic distances (Å) and angles (°)

M(1)		
1 M(1)–O(7)	2.049	
1 M(1)–O(10)	2.080	
1 M(1)–O(1)	2.101	
2 M(1)–O(4)	2.117	
1 M(1)–O(5)	2.225	
Mean	2.115	
1 O(5)–O(7)*	2.511	71.81
2 O(1)–O(4)**	2.561	74.79
1 O(1)–O(5)**	2.630	74.82
1 O(7)–O(10)	2.974	92.16
2 O(4)–O(10)	3.006	91.48
2 O(4)–O(5)	3.155	93.18
2 O(4)–O(7)	3.346	106.86
1 O(1)–O(10)	3.642	121.20
Mean	2.991	91.05
M(2)		
2 M(2)–O(3)	1.989	
2 M(2)–O(2)	2.064	
2 M(2)–O(8)	2.188	
Mean	2.080	
2 O(2)–O(3)**	2.604	79.94
4 O(2)–O(8)**	2.626	76.23
1 O(2)–O(2)$^{(4)}$	3.090	96.93
1 O(3)–O(3)$^{(4)}$	3.117	103.20
4 O(3)–O(8)	3.268	102.89
Mean	2.916	89.71
M(5)		
2 M(5)–O(2)	1.795	
2 M(5)–O(8)	1.952	
2 M(5)–O(6)	1.980	
Mean	1.909	
2 O(2)–O(6)**	2.525	83.79
1 O(8)–O(8)$^{(3)}$**	2.539	81.13
2 O(2)–O(8)**	2.626	88.90
1 O(6)–O(6)$^{(3)}$**	2.682	85.23
2 O(2)–O(8)$^{(3)}$	2.746	94.13
2 O(2)–O(6)$^{(3)}$	2.748	93.27
2 O(6)–O(8)	2.942	96.85
Mean	2.700	90.02
T(1)		
1 T(1)–O(3)	1.615	
2 T(1)–O(4)$^{(10)}$	1.618	
1 T(1)–O(9)$^{(10)}$	1.640	
Mean	1.623	
2 O(4)$^{(10)}$–O(9)$^{(10)}$	2.593	105.47
1 O(3)–O(9)$^{(10)}$	2.603	106.20
1 O(4)$^{(10)}$–O(4)$^{(11)}$	2.666	110.95
2 O(3)–O(4)$^{(10)}$	2.711	113.98
Mean	2.646	109.34
M(3)		
2 M(3)–O(1)	1.794	
2 M(3)–O(4)	1.878	
2 M(3)–O(6)	2.107	
Mean	1.926	
2 O(1)–O(4)**	2.561	88.45
2 O(1)–O(6)**	2.581	82.43
1 O(6)–O(6)$^{(3)}$**	2.682	79.03
2 O(1)–O(4)$^{(3)}$	2.759	97.42
2 O(1)–O(6)$^{(3)}$	2.784	90.69
1 O(4)–O(4)$^{(3)}$	2.824	97.51
2 O(4)–O(6)	2.865	91.73
Mean	2.717	89.83
M(4)		
1 M(4)–O(5)	1.820	
1 M(4)–O(3)	1.925	
1 M(4)–O(2)	1.954	
1 M(4)–O(1)	1.961	
2 M(4)–O(6)	2.098	
Mean	1.976	
2 O(2)–O(6)**	2.525	77.00
2 O(1)–O(6)**	2.581	78.90
1 O(2)–O(3)**	2.604	84.36
1 O(1)–O(5)**	2.630	88.08
1 O(3)–O(5)	2.712	92.77
1 O(1)–O(2)	2.882	94.79
2 O(5)–O(6)	3.083	103.61
2 O(3)–O(6)	3.103	100.88
Mean	2.784	90.06
T(2)		
1 T(2)–O(5)	1.612	
2 T(2)–O(6)$^{(10)}$	1.681	
1 T(2)–O(7)	1.697	
Mean	1.668	
1 O(5)–O(7)*	2.511	98.66
2 O(6)$^{(10)}$–O(7)	2.709	106.63
1 O(6)$^{(10)}$–O(6)$^{(11)}$	2.725	108.30
2 O(5)–O(6)$^{(10)}$	2.817	117.58
Mean	2.715	109.23
T(3)		
2 T(3)–O(7)	1.561	
2 T(3)–O(8)$^{(10)}$	1.621	
Mean	1.591	
4 O(7)–O(8)$^{(10)}$	2.577	108.15
1 O(8)$^{(10)}$–O(8)$^{(11)}$	2.631	108.50
1 O(7)–O(7)$^{(4)}$	2.644	114.72
Mean	2.597	109.30
X		
2 X–O(10)	2.071	
2 X–O(9)	2.286	
4 X–O(4)	2.628	
Mean	2.403	

Note: Under each atom heading are listed (X,M,T)–O bond distances and angles. Errors: M–O < 0.002 Å, O–O′ < 0.003 Å, angles O–M, T–O′ < 0.09°. Equivalent points are referred to Table 2 and appear as superscripts: (3) $x, -y, -z$; (4) $-x, y, z$; (10) $\frac{1}{2} - x, \frac{1}{2} - y, -z$; (11) $\frac{1}{2} - x, \frac{1}{2} - y, \frac{1}{2} + z$.

* Shared edge between M and T polyhedra.

** Shared edge between M and M′ polyhedra.

the value in Moore and Araki or Finger and Hazen and T to equal the value obtained in this study,

$$\Delta = [(W - T)/T] \times 100.$$

Mean values and their extrema are tabulated in Table 6. For three kornerupines from three different sources (two natural minerals, one synthetic), the similarities rather than the differences are surprising. The mean value of $|\Delta|$ for all U_{ii} of the 8-cation and 10-anion unique positions is a little over 25% for cations and a little under 17% for anions. Cations usually give larger Δ values than anions, a consequence of smaller thermal motion for the cations and of more variegated solid solution in these cation positions. The greatest deviants, +156.2% for T(3) of Moore and Araki (1979) and +141.0% for M(2) of Finger and Hazen (1980) arise in part from the arithmetic involved; since the U_{ii} individual values employed the relatively small values in this study as the divisor, such differences appear exaggerated, at least in the condensed manner by which we express them.

The average B_{eq} are also listed. The match is remarkably close, within 20% for cations and 3% for anions. These

Table 6. Refined kornerupines: Differences in thermal parameters

Ref.	ΔU_{ii} (i = 1 to 3) Mean	ΔU_{ii} (i = 1 to 3) Extrema	ΔB_{eq} Mean	ΔB_{eq} Extrema
		A. M(1)–M(5) and T(1)–T(3)		
MA	30.2	−16.2 for T(2) to +156.2 for T(3)	20.8	−0.0 for M(3) to +88.9 for T(3)
FH	32.1	−32.5 for M(4) to +141.0 for M(2)	23.0	−23.1 for M(4) to +72.5 for M(2)
		B. O(1)–O(10)		
MA	15.9	−27.5 for O(10) to +69.0 for O(4)	9.4	−21.3 for O(10) to +14.1 for O(4)
FH	25.9	−40.5 for O(7) to +88.1 for O(4)	15.6	−20.6 for O(7) to +22.7 for O(2)
		C. Mean of $\lvert\Delta\rvert$ for M(1)–M(5), T(1)–T(3), and O(1)–O(10)		
MA	22.2		14.5	
FH	28.6		18.9	

	M(1)–M(5)	T(1)–T(3)	O(1)–O(10)
	D. Mean B_{eq} (Å²)		
TS	0.53	0.46	0.77
MA	0.59	0.59	0.77
FH	0.61	0.47	0.79

Note: All calculations refer to values in the present study.

Part A is for cations, Part B is for anions, and Part C is for all 18 occupied atoms in the asymmetric unit. Mean values of the difference magnitudes, $\lvert\Delta\rvert$, and individual extreme points are also given in percent. These values are given for U_{ii} (i = 1 to 3) and B_{eq}. Part D lists the mean equivalent isotropic thermal parameters.

* References: MA—Moore and Araki (1979); FH—Finger and Hazen (1980); TS—this study.

similar results from three independent studies underline the importance of assessing thermal-vibration parameters in evaluating the "correctness" of a structure.

When a structure is accurately known, it is desirable to calculate individual deviations from bond-distance averages and compare them with deviations in electrostatic neutrality. The simple Pauling model was adopted, mainly because it does not masquerade deviations but proceeds directly from formal charges, coordination numbers, and individual distance deviations calculated directly from Table 4. Individual bond strengths, s, were calculated for a purely ionic model and from the cation-site populations and coordination numbers discussed earlier. Calculated deviations from $p_0 = 2.00$ for O^{2-} and individual distance deviations are listed in Table 7. Only O(10) has attached H and the O–H bond was given $s = 5/6$ suggested by Baur (1970). The centroid of the H atom could not be located in our difference synthesis. However, it was postulated by Moore and Araki (1979) that a series $X^{2+}_{\frac{2}{3}}\square_{\frac{1}{3}}OH^{-}$–$X^{2+}_{1}O^{2-}$ existed. This can now be tested to some degree.

Thirty-six entries occur in Table 7, and of these, six violate the expected bond length–bond strength relationships. In other words, 83% of the values are in concord. Five of the six values involve X and M(1), the two most distorted polyhedra in the structure. The violations involve the anions O(4), O(5), O(7), and O(9) of which O(7) and O(9) have undersaturated values for these entries. The O(4), O(5), and O(7) are eliminated as they involve shared edges with other fully populated polyhedra, that is, their distances are too long, owing to cation-cation repulsion effects. The O–H(10)···O(9) distance of 2.763(3) Å corresponds to a shared edge between two $XO(4)_4O(9)_2O(10)_2$ distorted cubes. If a successive pair of such cubes has unoccupied X, the O–H(10)···O(9) hydrogen bond is possible. The *increase* in X occupancy would require a *decrease* in H content, suggested earlier by the postulated $X^{2+}_{\frac{2}{3}}\square_{\frac{1}{3}}OH^{-}$–$X^{2+}_{1}O^{2-}$ series. However, the left side of the equation is not balanced, and quantitative presence of hydroxyl groups would not be possible in this model owing to shared edges with occupied cubes. A more reasonable

Table 7. Kornerupine: Electrostatic valence balance of cations and anions

Anions	Cations X	M(1)	M(2)	M(3)	M(4)	M(5)	T(1)	T(2)	T(3)	Δp_0
O(1)	—	−0.01	—	−0.13, −0.13	−0.01	—	—	—	—	−0.17
O(2)	—	—	−0.03	—	−0.02	−0.11, −0.11	—	—	—	−0.17
O(3)	—	—	−0.11	—	−0.05	—	−0.01	—	—	−0.17
O(4)	*+0.22*	*+0.00*	—	−0.05	—	—	−0.00	—	—	−0.07
O(5)	—	*+0.11*	—	—	−0.15	—	—	−0.06	—	−0.23
O(6)	—	—	—	+0.18	+0.12	+0.07	—	+0.02	—	+0.44
O(7)	—	*−0.07*	—	—	—	—	—	+0.03	*−0.03*	+0.17
O(8)	—	—	+0.14	—	—	+0.04, +0.04	—	—	+0.03	+0.23
O(9)	*−0.11*	—	—	—	—	—	+0.01, +0.01	—	—	+0.19
O(10)	−0.33, −0.33	−0.03, −0.03	—	—	—	—	—	—	—	−0.32

Note: Bond length–bond strength contradictions are in italics. Entries are individual deviations from polyhedral averages (Table 4).

Table 8. Comparison of Ni_2In, olivine, and kornerupine

Ni_2In	a_0(N) = 4.18	b_0(N) = 7.24	c_0(N) = 5.13	*Cmcm*
Olivine	*a*(F) = 4.76	*b*(F) = 10.22	*c*(F) = 5.99	*Pbnm*
Kornerupine	*a*(K) = *a*/5 = 3.21	*b*(K) = 13.75	*c*(K) = 6.72	*Cmcm*

Note: Values are in angstroms.

series on the left side would be $X^{2+}_{1/3}\square_{1/3}OH^{-}_{1/3}$. This stoichiometry appears to fit our refined structure fairly well.

Finally, bond distances in Table 4 can be addressed. The polyhedral distortions resulting from shared edges are in perfect agreement with predicted results, the sole T(2)–$O^{(3)}_{(7)}$–M(1) tetrahedral-octahedral shared edge being the shortest for all the polyhedra.

Kornerupine: Structural principles

Since Moore and Bennett (1968) first reported the crystal structure of kornerupine, Moore and Araki (1979) refined data from a B-rich synthetic crystal, and Finger and Hazen (1980) refined a Fe-rich member, but little insight has been gained on the crystal-chemical principles of this complex structure type. This is especially embarrassing since the structure type has been turning up in many terranes of granulite facies. All attempts to derive its structure from hexagonal and/or cubic dense-packed oxide anions have failed. Both the first and second structure studies stressed principles of anion close-packing in *sections* of the crystal structure, from a projection along [001] in the first study and along [010] in the second. Yet the packing efficiency of 16.8 Å^3 per O^{2-}, when compared with $4\sqrt{2}\,r^3$ = 15.52 Å^3 for the "classic" Pauling O^{2-} radius r = 1.40 Å, suggested a dense-packed structure. Such packing, however, does not necessarily imply cubic or hexagonal close-packing: many very dense-packed structure types (glaserite, $K_3NaS_2O_8$; or garnet, $Mg_3Al_2Si_3O_{12}$, for example) do not belong to these simple packing principles. For such structures, we have had considerable success through seeking out analogies between cations in the oxysalts and atomic positions in intermetallics. This approach largely stems from the penetrating study of O'Keeffe and Hyde (1985), where they discussed isopunctal relationships comparing cations in garnet with Cr_3Si, cations in olivine with Ni_2In, the apatite structure type with Mn_5Si_3 and many other analogies. Incidentally, glaserite's cations can be directly related by comparing the cations of $(K_3NaS_2)O_8$ to Ni_4In_2 and those of the långbanite monstrosity with americium, $\cdot ch\cdot$!

A general formula can be written for kornerupine, where M are cations in octahedral and higher coordination by oxide anions, T are tetrahedrally coordinated cations, and ϕ corresponds to generalized anion. Including the large, partly occupied X site, kornerupine has $M_{40}T_{20}\phi_{88}$ for the unit-cell contents. If the cations only are projected along the three principal crystallographic axes, a quite different picture from the earlier studies is immediately recognizable. All nine cations in the asymmetric unit define three distinct rods, each made up of three unique cations when projected along the [100] direction. When the mirror plane normal to the *a* axis at $x = 0$ is included, five beads of cations are created per rod for one cell translation. Each unique rod is given a symbol: M(a) at *x*, 0, 0; M(b) at *x*, 1/6, 1/4; and T at *x*, ~1/3, 1/4. It is noted that the beads are separated by intervals of approximately *x*/5 along the direction of projection. The separation, Δ, of beads in each rod in the projection (*y*-*z* plane) are within Δ = 0.0 for M(a), 0.1 for M(b), and 0.3 Å for T.

The orthogonalized cell and its atom positions for Ni_2In can be directly related. That is, $P6_3/mmc$, *a*(h) = 4.179, *c*(h) = 5.131 Å (Laves and Wallbaum, 1942), 2 In(1/3 2/3 1/4); 2 Ni(1) (0 0 0); 2 Ni(2) (1/3 2/3 3/4) → *Cmcm*, a_0 = 4.18, $b_0 = a(h)\sqrt{3}$ = 7.24, c_0 = 5.13 Å; 4 In(0 1/3 1/4); 4 Ni(1) (0 0 0); 4 Ni(2) (1/2 1/6 1/4). Thus, we can compare the average cation or metal positions in the *y*-*z* plane: (0.343, 1/4), (0.333, 1/4) for T, In; (0, 0), (0, 0) for M(a), Ni(1); and (0.142, 1/4), (0.167, 1/4) for M(b), Ni(2). The displacements in the *y*-*z* plane are Δ = 0.16, 0.00, and 0.40 Å, respectively, when computed on the kornerupine unit cell.

Kornerupine's cations track very nicely on Ni_2In positions along [100]. Therefore, the comparison among Ni_2In, olivine, and kornerupine is a very anisotropic relation, indeed, as shown in Table 8. Can these relative anisotropies be explained? From this prelude, a fugue is now required.

But discussion on correlations among cations or metals in kornerupine, olivine, and Ni_2In hardly explains the extreme anisotropy among equivalent cell translations, and the role of the electronegative oxides must also be discussed. It would be most desirable to seek an intermetallic cluster or molecule with well-defined geometry and to examine the locations of and distortions created by oxygen insertion. From this model, which involves a finite cluster, an extension to infinitely extending arrays is possible *so long as all atoms in the asymmetric unit can be counted and so long as the electron count is preserved.*

Such a model exists and illustrates the insertion of oxygen into an intermetallic, in this case one of the polymorphs of phosphorus, P_4 or white phosphorus. Figure 1 shows the progression $[P_4]$, $[P_4O_6]$, and $[P_4O_{10}]$, the same sequence as featured in Wells (1975). Errors in distances reported for these three structure determinations each are about ±0.03 Å. In the $[P_4]$ tetrahedron, the P–P edge (bond pair) is 2.21 Å. This value was established by electron diffraction off a jet of P_4 vapor (Maxwell et al., 1935). From the model, each vertex is 3-connected, and each P contributes three electrons to bond-pair formation and

two electrons to the terminal electron lone pair, ψ. Since P has five valence electrons ($3s^2 3p^3$), the package $[P_4\psi_4]$ has six bond pairs and four lone pairs, thus accounting for all $5 \times 4 = 20$ valence electrons for $[P_4]$.

Now in $[P_4O_6]$, six oxygens are inserted near the midpoints of the P–P edges. Since the more electronegative oxygen has six valence electrons ($2s^2 2p^4$), two more electrons are required for Lewis octet closure. In fact, Lewis octets constitute a hallmark of twentieth century science, both in crystals and in other condensed states (Lewis, 1916). Octet closure is achieved by the P–P bond pairs at the midpoints of the six edges that incorporate the six oxygens. The P–O distances are 1.65 Å, and the P–P distance is expanded to 2.95 Å. This experiment also employed electron diffraction of jets, reported by Hampson and Stosick (1938). The terminal positions from the P atoms still remain electron lone pairs, and the molecule can be expressed as $[P_4O_6\psi_4]$. The midpoint of the P–P distance was expressed in atomic coordinates for the purported locus of the bond pair. The distance d between this midpoint and the centroid for the adjacent oxygen computed to be 0.74 Å. These distances are shown in Figure 1.

Finally, in P_4O_{10}, the four terminal lone pairs complete the octets of four terminal oxygens. Its structure was derived from an X-ray diffraction experiment earlier conducted by de Decker and MacGillavry (1941), later refined by Cruickshank (1964) who reported average distances for P–O (bridging) of 1.60 Å and for P–O (terminal) of 1.40 Å. These differences can be easily understood from Pauling's rules, the bridging oxygen being oversaturated ($\Delta p_0 = +0.50$ valence units) and the terminal oxygen being undersaturated ($\Delta p_0 = -0.75$ v.u.) by bonded P atoms. The P–P distance of 2.79 Å is an average of two independent but very similar distances. The average distance between the midpoint of P–P and the centroid for adjacent oxygen is $d = 0.78$ Å. Thus, the progression $[P_4\psi_4] \rightarrow [P_4O_6\psi_4] \rightarrow [P_4O_{10}]$ exploits the Lewis octet formation about the most electronegative species, oxygen. Note that in the progression in Figure 1, the inserted oxygens are at approximate midpoints of P–P edges and displaced somewhat outward from these edges in the tetrahedron. The expansion of P–P is considerable: for P_4O_6, the P–P dilation is $\Delta = +25\%$, and in P_4O_{10} it is $\Delta = +21\%$ with respect to P_4. In these calculations and those that follow, the dividend is the difference between the oxysalt and the intermetallic values being compared. The divisor is the oxysalt value, and the quotient is multiplied by 100 and rounded off to the nearest whole number. The result is expressed in *linear* measure by extracting the cube root of volume per metal atom, which was derived from the crystallographic unit cell.

O'Keeffe and Hyde (1985, especially p. 99) discussed linear and volumetric changes in some detail and stressed that dilation does not necessarily follow in the progression $M_aT_b \rightarrow M_aT_b\phi_a$ where M and T are metals and ϕ the electronegative anion, usually O^{2-}. They declared, "Although there is often a considerable volume increase on forming an inorganic structure from the corresponding

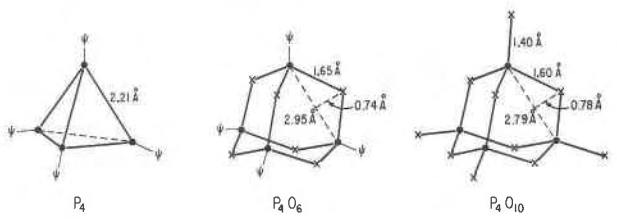

Fig. 1. Spoke diagrams for $[P_4]$, $[P_4O_6]$, and $[P_4O_{10}]$. ● = P atoms, X = the oxygen centroids, and ψ = the lone pairs of electrons. Key distances are given.

alloy 'by (notionally) inserting anions into the latter' . . . ," exceptions abound. This can be demonstrated in Table 9 where examples of well-defined oxysalt-metal pairs have been selected from Villars and Calvert (1985) and Donnay and Donnay (1963). The seven pairs include binary oxides in the system MgO-Al_2O_3-SiO_2, which encompasses most of kornerupine. Note that five oxysalt-metal pairs in Table 9 exhibit the same cation or metal *eutaxy* (= "well-arranged") but two MgO-Mg and Al_2O_3-Al do not, although their structures are based on principles of close-packing. We found the most convenient way to relate the pairs involves calculations of cell volume per metal for each pair, then taking the cube root of these values to get a linear expression as percent change, which was earlier discussed.

In Table 9, the valence electrons are listed as well, and the table is arrayed according to increasing electron populations of the orbitals. A trend immediately becomes obvious. The top three entries with only ns^2 valence electrons for the metals *decrease* in volume for Me → MeO. Note that the Ca → CaF_2, $\Delta = -2\%$ compared with Ca → CaO, $\Delta = -16\%$. It is believed that an aliquot of twice the number of fluoride ions compared with oxide ions for the isopunctal Ca metals accounts for this difference. The remaining five pairs *increase* in volume for Me → MeO. These pairs include additional p- and d-electron populations. This contrast appears easily explained by Pauling (1960, p. 110): "*p bonds are stronger than s bonds*" and "it is convenient to call the magnitude of a bond orbital in its angular dependence the *strength* of the bond orbital, with value 1 for an s orbital and 1.732 for a p orbital."

Since kornerupine is constructed principally of Al_2O_3 and SiO_2 components with somewhat less MgO, it follows that the kornerupine cell will *expand* with addition of electronegative oxide ions relative to its chemical equivalent of the Ni_2In intermetallic.

The $[P_4]$ cluster model above was applied directly to the complex kornerupine crystal structure. In every respect, the same calculations were performed. This required taking all the countable cation-cation positions, to determine the midpoints of their connections and to calculate the distance between each midpoint with respect to its adjacent oxide centroid. The midpoint is suggested by the $[P_4O_6\psi_4]$ and $[P_4O_{10}]$ molecules where $d \approx 0.76$ Å occurs on the average between adjacent oxide centroid

Table 9. Kornerupine components and some oxysalt-metal relations

	A	B	C	D
1.	$\frac{MgO-Mg}{MgO}$	*Fm*3*m* vs. $P6_3/mmc$	$3s^2$	−7%
2.	$\frac{*CaO-*Ca}{*CaO}$	*Fm*3*m* vs. *Fm*3*m*	$4s^2$	−16%
3.	$\frac{*CaF_2-*Ca}{*CaF_2}$	*Fm*3*m* vs. *Fm*3*m*	$4s^2$	−2%
4.	$\frac{½Al_2O_3-Al}{½Al_2O_3}$	$R\bar{3}c$ vs. *Fm*3*m*	$3s^23p$	+8%
5.	$\frac{*SiO_2-*Si}{*SiO_2}$	*Fd*3*m* vs. *Fd*3*m*	$3s^23p^2$	+24%
6.	$\frac{*CoO-*Co}{*CoO}$	*Fm*3*m* vs. *Fm*3*m*	$3d^74s^2$	+16%
7.	$\frac{*NiO-*Ni}{*NiO}$	*Fm*3*m* vs. *Fm*3*m*	$3d^84s^2$	+16%

Note: Starred metals are in isopunctal relationship. Col. A: oxysalt and metal pairs used in volumetric calculations. Col. B: space groups of oxysalt vs. metal. Col. C: valence electrons for metal. Col. D: linear change or cube root of volume per metal (Å^3, based on unit cell) for oxysalt-metal pairs. Nos. 1, 4, and 5 from Villars and Calvert (1985); 2, 3, 6, and 7 are from Donnay and Donnay (1963).

and the P–P centroid. Calculations that ensue always take the midpoint of two adjacent cations as the locus of the bond pair.

But kornerupine is an extended three-dimensional structure. How are the cations counted? Unconventional diagrams in Figure 2 are presented for both kornerupine and olivine where emphasis is placed on cation coordination about anions. Note that O(1), O(2), O(4), O(6), O(8), O(9), and O(10) are each four-coordinated and define rather distorted tetrahedra and O(3), O(5), and O(7) are each three-coordinated by cations that define distorted triangles. The olivine map also reveals four-coordination of cations about anions, in each case three octahedral (M = Mg) and one tetrahedral (T = Si) cation. In both cases, the maps appear rather cumbrous, but much information is given in them: they are more extended equivalents of the [P_4] sequence. Since *Pbnm* (olivine) ⊂ *Cmcm* (kornerupine), both structures were projected along the *z* direction, the shortest translation in kornerupine. Only anions within $0 \leq z \leq ½$ are shown in order to minimize redundancy and congestion. The olivine and Ni_2In cells were scaled to conform with kornerupine for purposes of comparison. Heights in *z* are given as fractional coordinates. Anions are shown as filled squares, and cations as solid disks; the scaled Ni(1), Ni(2), and In centroids for the Ni_2In intermetallic are shown as crosses. Dashed lines in Figure 2 have the same connotation as those for the [P_4] series in Figure 1, that is, a dash between the cation pair, and a dash from the adjacent anion to this pair. In addition to many of the *d* values (the distance between cation-cation midpoint and adjacent anion) in the figures, cation deviations between oxysalt and intermetallic are given in angstroms, as are the *d* values between oxide centroids and cation-cation midpoints listed in Table 10.

To make sure all cations and anions were represented, graphs (of which there are many choices) from Figure 2 were constructed. The collection used here for kornerupine includes two chain segments: –M(5)–O(2)–M(5)–O(6)–T(2)–O(5)–M(4)– and –M(1)–O(10)–M(1)–O(7)–T(3)–O(8)–M(2)–O(3)–T(1)–O(9)–T(1)–O(4)–M(3)–O(1)–M(3)– . Since all anions are listed, the formation of Lewis octets can be achieved. Clearly, many other combinations can be written, as each anion is either three-coordinated or four-coordinated by cations, but this doesn't matter since we are only required to seek out bond pairs associated with anions for potential Lewis octet closure. Segments of these chains occur in Table 10, compared with the Ni_2In intermetallic, and the distance *d* between cation-cation edge midpoint and oxide centroid is entered. The range is $d = 0.21$ Å for O(5) to 0.96 Å for O(6) with a mean of 0.68 Å for all oxygens. For olivine, the range is 0.88 Å for O(3) to 0.99 Å for O(1) with a mean of 0.93 Å. It is obvious that kornerupine more closely mimics the Ni_2In arrangement than does olivine, as shown by a model for the olivine arrangement by O'Keeffe and Hyde (1985). An equally important calculation is the difference, Δ (Å), between ideal and real atomic coordinates for kornerupine, olivine, and Ni_2In. In Table 2 it is seen that the mean is 0.26 Å for kornerupine (range 0.00 to 0.50 Å) and 0.46 Å for olivine (range 0.00 to 0.82 Å). Yet again, kornerupine, even with its relatively large number of atoms in the asymmetric unit, shows the best correspondence with the intermetallic. The space groups of the latter pair are the same, *Cmcm*. Note that a nearly regular subcell occurs for kornerupine with $a(N) \approx a/5(K)$ that was automatically included in calculating the cation (metal) positions between these two structures.

The X cation in kornerupine and the M(1) cation in olivine are the only atoms not represented for these structures in Table 10. Attempts were made to find reasonable graphical connections, but these were either too long, or the ensuing *d* values were too large. It appeared that X and M(1) played somewhat different roles in the structures than in corresponding Ni_2In. It is interesting to note that these sites play anomalous roles in the structures: X is only partially occupied in kornerupine, and M(1) in olivine, which experiences similar disorder, is the basis of omission derivative structures such as sarcopside, heterosite, and laihunite.

Kornerupine, olivine, and Ni_2In: Similarities and cell anisotropies. Emphasis in Tables 2, 9, and 10 and in Figure 2 has been placed on the similarities of cation positions among these three structure types. For example, in Table 2, it is seen that X, M(1)–M(5), and T(1)–T(3) in kornerupine and M(1), M(2), and T in olivine (forsterite) correspond to Ni(1), Ni(2), and In in Ni_2In. The relation X,M → Ni and T → In is hardly an accident! If such a correspondence occurs, then why do the cell shapes markedly differ? As before, for proper comparison, the *a* axis of kornerupine must be partitioned into its subcell $a' = a/5$. Figure 2 presents the general relationships among the cations and their correspondence in these structures. For

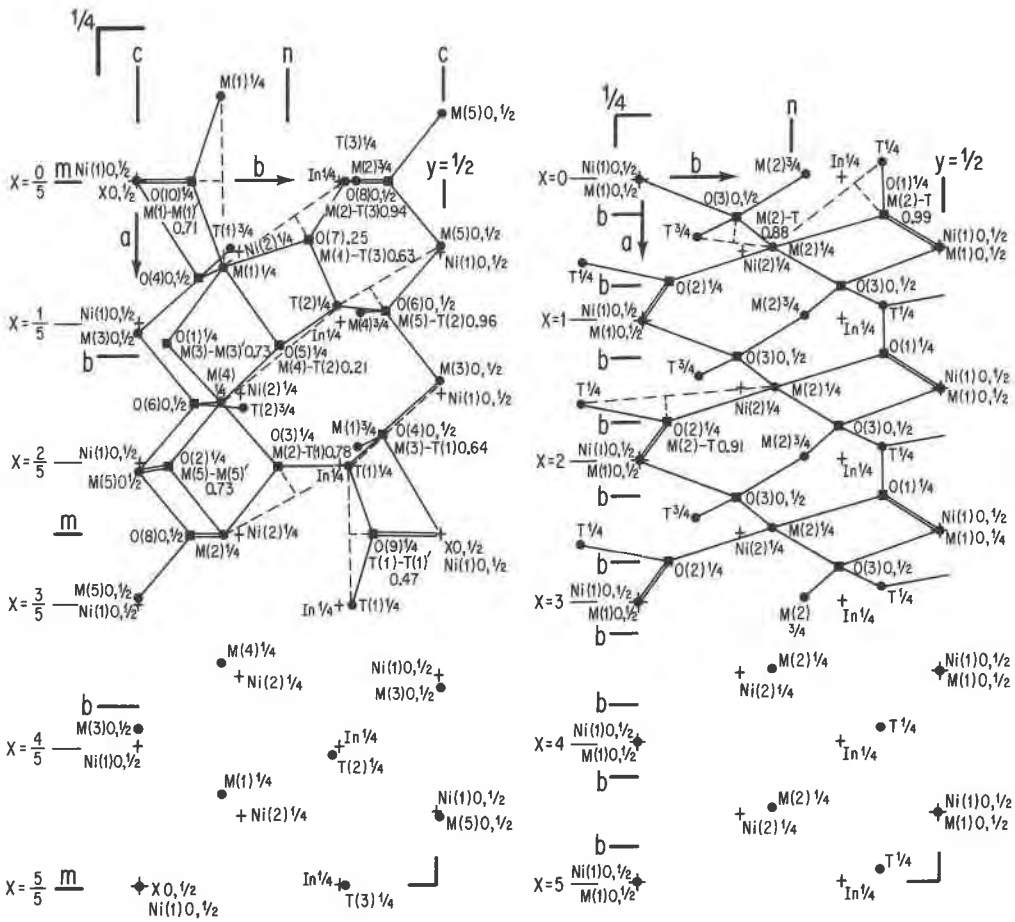

Fig. 2. Spoke diagrams of kornerupine on left and olivine scaled to kornerupine cell on right. Cell origins and outlines of projection along [001] are designated by arrows and right angles. Most atoms are $0 \leq z \leq \frac{1}{2}$. Heights in fractional coordinates, cations as circles, anions as squares, Ni_2In as crosses, translations in x on left. Some symmetry elements are shown. Dashed lines have same connotation as in Fig. 1. Displacements in Å from midpoints of cation pair to nearest anion are given under that anion. The lower portions of both maps show cation and Ni_2In centroids only. This is a map of cations about anions. Note three-coordination for O(3), O(5), and O(7), and four-coordination for O(1), O(2), O(4), O(6), O(8), O(9), and O(10).

convenience, set t_i, $i = 1$ to 3, as the unit-cell translations a (or $a/5$ in kornerupine), b, and c. The orthohexagonal cell for Ni_2In has been already defined. Its contents are $4Ni_2In$, and the cell translations and axial ratios are listed in Table 11.

It is immediately recognized that the ratios indicate extensive cell anisotropy among these compounds. We believe that this can be explained by the rather anisotropic insertion of the oxygen atoms. Recalling the sequence $[P_4] \rightarrow [P_4O_6] \rightarrow [P_4O_{10}]$ with a linear increase of some 25%, note that in Figure 1 the oxygen insertions can also be considered as insertions of layers or planes that lie between but do not anywhere include cations. In cubic structures, we saw that dilation was uniform in three dimensions. Analogous to the tetrahedral $[P_4]$ sequence, such planes would be parallel to $\{\bar{1}\bar{1}\bar{1}\}$ for example. In orthorhombic crystals, orientation of added oxygen layers according to $\{100\}$, $\{010\}$, $\{001\}$, or $\{110\}$, etc., would lead to marked anisotropy in axial ratios compared with the intermetallic; the anisotropy would be particularly pronounced normal to that layer receiving the extra insertions. Any "isotropic" insertion for an orthorhombic intermetallic would lead to a compound with closely similar axial ratios.

It is believed that the adjusted axial ratios in Table 11 best explain the anisotropy through oxygen insertion and bond-pair formation. Through trial and error, the best axial direction was selected, and the standard ratios were scaled according to the axial ratio for Ni_2In. These are listed in parentheses. Here, c for kornerupine and a for olivine were set according to Ni_2In. For kornerupine, we see a decrease in a by about 42% and an increase in b by about 45%. In olivine, a and c are similar to the Ni_2In ratios, but b is increased by about 24%. In kornerupine, anions O(1)–O(8) all contribute to laminae between X and

TABLE 10. Kornerupine and olivine: Displacements between cation pairs and adjacent anions

Anion	Adjacent cation pair†	N_2In atoms	Distance (Å)	Displacement‡ (Å)
		Kornerupine		
O(1)	*M(3)–M(3)′	Ni(1)–Ni(1)	2.57	0.73
O(2)	*M(5)–M(5)′	Ni(1)–Ni(1)	2.57	0.73
O(3)	ˣT(1)–M(2)	In–Ni(2)	2.41	0.78
O(4)	ᵛT(1)–M(3)	In–Ni(1)	2.73	0.64
O(5)	ˣT(2)–M(4)	In–Ni(2)	2.41	0.21
O(6)	ᵛT(2)–M(5)	In–Ni(1)	2.73	0.96
O(7)	ˣT(3)–M(1)	In–Ni(2)	2.41	0.63
O(8)	*T(3)–M(2)	In–Ni(2)′	2.57	0.94
O(9)	□T(1)–T(1)	In–In	4.18	0.47
O(10)	□M(1)–M(1)	Ni(2)–Ni(2)	4.18	0.71
Mean				0.68
		Olivine		
O(1)	ˣT–M(2)	In–Ni(2)	2.41	0.99
O(2)	ˣT–M(2)	In–Ni(2)	2.41	0.91
O(3)	*T–M(2)	In–Ni(2)′	2.57	0.88
Mean				0.93

† Orientations of pairs: □ parallel *a*, * parallel *c*, X in *a-b* plane V in *a-b-c* plane.
‡ The displacement (*d*) between cation-pair centroid and adjacent anion.

M(1)–M(5) cations to form edge-sharing chains parallel to [100]. This

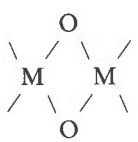

sequence defines oxygen insertions where no bonds occur in Ni_2In (the a = 4.18 Å translation; see below)! This wholesale formation of bond pairs results in M–M ≈ 3.2 Å. The big increase along b is also explained by the anion insertion. Laminae of O(4), O(6), O(8), O(9), and O(10) parallel to {010} are inserted nearly *between* atom bond pairs and are located near $y \approx \pm(1/8, 3/8)$. Additional laminae of O(3), O(5), and O(7) also parallel to {010} are located near $y \approx \pm(2/8)$. Kornerupine is a particularly interesting example where both bond-pair formation and anion-layer insertion have a ready explanation in the axial ratios. This is admittedly a qualitative model, and neither all bond pairs nor all anions were accounted for. As yet, a quantitative model has not been perfected. In such an event, many exciting new discoveries will be made, especially "turning intermetallics into oxysalts." The best display of this remarkable structure is either projection along [001] or deciphering the diagrams in Moore and Bennett (1968) and Moore and Araki (1979).

Olivine poses similar problems. Its cell parameters and axial ratios suggest that the most anisotropic increase is along b with an increase of about 24% with respect to Ni_2In. Unlike kornerupine, all anions form bond pairs nearly between the bond pairs in Ni_2In. In olivine there are no additional insertions (as occur for kornerupine) between nonbonded regions for Ni_2In. The only anion to

TABLE 11. Cell translations and axial ratios

	t_1	t_2	t_3	Axial ratio	Adjusted axial ratio
Ni_2In (N)	4.18	7.24	5.13	0.577:1:0.708	
Korn (K)	3.21	13.75	6.72	0.233:1:0.489	(0.337:1.448:0.708)
Forst (F)	4.76	10.22	5.99	0.466:1:0.586	(0.577:1.238:0.726)

form laminae *between* the cations is O(3) in a general position. The M(2) and Si cations on either side of the O(3) laminae parallel to {010} are displaced themselves, accounting for the greater difference between atoms in the intermetallic and cations in olivine in Table 2. While in Ni_2In, the displacement in the a-b plane is 0.00 Å, the corresponding M(2)–Si in olivine is displaced ~1.3 Å.

Table 12 summarizes the chemical crystallography and bond nomenclature for Ni_2In and α-Fe. Just as it is proposed that Ni_2In forms the atomic basis of cation distributions in kornerupine and olivine, so Ni_2In is an ordered derivative of α-Fe. The element has $z = 2$, $Im\bar{3}m$, a = 2.866 Å (Donnay and Donnay, 1963). Selecting the hexagonal cell for α-Fe, a direct comparison can be made as outlined in Table 12. Partitioning Fe into three equivalences yields the ordering scheme compared with Ni_2In, also given in Table 12. The maximum difference between equivalences is Δ = 0.43 Å based on the c axis of Ni_2In. With differences in electronegativities and bonding, we believe Ni_2In can be considered an ordered pseudoderivative structure of α-Fe. The prefix *pseudo* is used because $R\bar{3}2/c$ and $P6_3/mmc$ share same cell but not same class relationships.

Included in Table 12 are the metal-metal distances for Ni_2In, the number of equivalent bonds, the planes that include them (based on the orthohexagonal a_0, b_0, c_0) and a code (1–2, 3–3a, 4–4c, 5–5b) for the kinds of bonds. The $In[Ni_{11}]$ and $Ni(2)[In_5Ni_6]$ define distorted pentacapped trigonal prisms and $Ni(1)[In_6Ni_8]$, a bicapped hexagonal prism. These bonds are found among the cation-cation distances in kornerupine and olivine. The 5–5b distances of a_0 = 4.18 Å each are not bonded. They play a central role in kornerupine as discussed earlier.

Taken together, the kinds of bonds, their number in the olivine, and one-fifth the kornerupine cell (the unit for comparison) are as given in Table 13. The differences arise from bond arrangements of varying distribution, an "olivine" stoichiometry of $M_2TO_{4.4}$ in kornerupine, and the appearance of three-coordination of cations about anions O(3), O(5), and O(7) in the latter mineral.

It is now possible to address the intriguing question: can Table 9 serve as a vehicle to compare the linear change for oxysalt-metal pairs associated with kornerupine and with olivine? An interesting twist is added to the problem, for here not single components (such as $\frac{1}{2}Al_2O_3$ and Al) but several components are involved. Several assumptions are made, some of which were assumed before: (1) the single components are based on principles of close-packing, either $\cdot c \cdot$, $\cdot h \cdot$ or combinations of these. For perfect spheres, there is no change in packing efficiency,

Table 12. The Ni_2In and α-Fe intermetallics: Chemical crystallography

Ni_2In				α-Fe			
$P6_3/mmc$				$Im3m$ $(R\bar{3}2/c)$			
2 Ni_2In				2 Fe 0 0 0 a = 2.866 Å			
a = 4.179	c = 5.131 Å	c/a = 1.228		a(h) = $\sqrt{2}a$ = 4.052	c(h) = $\sqrt{3}a$ = 4.964 Å	c(h)/a(h) = 1.225	
a_0 = 4.179	$b_0 = a\sqrt{3}$ = 7.238	c_0 = 5.131 Å		a_0 = 4.052	b_0 = 7.018	c_0 = 4.964 Å	
2 In	⅓	⅔	¼	2 Fe(a)	⅓	⅔	⅙
2 Ni(1)	0	0	0	2 Fe(b)	0	0	0
2 Ni(2)	⅓	⅔	¾	2 Fe(c)	⅓	⅔	⅚

	(Å)				
1 In–Ni(2)	2.41			b_0	1
2 In–Ni(2)′	2.41			a_0b_0	2
2 In–Ni(2)″	2.57			c_0	3
4 In–Ni(1)	2.73			$a_0b_0c_0$	4
2 In–Ni(1)′	2.73			b_0c_0	4b
	11 pentacapped trigonal prism				
2 Ni(1)–Ni(1)′	2.57	c_0	3a	1 Ni(2)–In	2.41	b_0	1
2 Ni(1)–Ni(2)	2.73	b_0c_0	4c	2 Ni(2)–In′	2.41	a_0b_0	2
4 Ni(1)–Ni(2)′	2.73	$a_0b_0c_0$	4a	2 Ni(2)–In″	2.57	c_0	3
2 Ni(1)–In	2.73	b_0c_0	4b	4 Ni(2)–Ni(1)′	2.73	$a_0b_0c_0$	4a
4 Ni(1)–In	2.73	$a_0b_0c_0$	4	2 Ni(2)–Ni(1)	2.73	b_0c_0	4c
	14 bicapped hexagonal prism				11 pentacapped trigonal prism		
2 In–In′	4.18			a_0			5
2 Ni(2)–Ni(2)′	4.18			a_0			5a
2 Ni(1)–Ni(1)′	4.18			a_0			5b

Note: In computed bond distances, axes that include these bonds and a code (1–5) are included. Nonbonded distances appear at end.

V_E, or volume per atom. (2) The volumetric differences in types of close-packing among crystals of same composition are negligible. (3) A phase composition, whether real or hypothetical, involving more than one component can be evaluated by a principle of additivity, i.e., the sum over all components in its formula. This implies additivity of the volumes of each of the components in the formula unit.

The cell formula for olivine is $4Mg_2SiO_4$, the X-ray cell volume V = 291.86 Å^3 from Birle et al. (1968) for forsterite. In the same manner as deriving Table 9, Mg_2Si is 8Mg + 4Si = 184.81 Å^3 + 80.10 Å^3 or 264.91 Å^3. The volume change from intermetallic to oxide is

$$[(291.86 - 264.91)/291.86] \times 100 = +9.2\%.$$

The average *linear* increase is

$$\Delta = [(6.633 - 6.422)/6.633] \times 100 = +3.2\%.$$

This value can be compared with column D in Table 9. The valence electrons for the metals are $3s^2$ and $3s^2p^2$, and the small net linear increase is believed to reflect Pauling's (1960) estimates of relative bond strengths of s and p bonds. Kornerupine with a greater aliquot of p bonds would be expected to expand even more than olivine, when compared with its metal components.

To appraise this effect in kornerupine, the formula derived from Scoon in McKie (1965) was simplified from eight components to the three major components. These three major components in the Scoon analysis add to MgO + Al_2O_3 + SiO_2 = 93.32%, the remaining 6.68% being principally Fe_2O_3 and B_2O_3. Good oxysalt-metal pairs could not be obtained for these two components. In addition, their small contribution was deemed insignificant, and this 6.68% remainder was added to Al_2O_3. The three-component "analysis" computed to an olivine-related formula $(5.461 \times 4)Mg_{0.677}Al_{1.310}Si_{0.679}O_{4.000}$, the prefix scaling it to kornerupine cell contents. The X-ray cell volume is V = 1480.65 Å^3. That for only the metals (5.461 × 4)(0.677Mg + 1.310Al + 0.679Si) from Table 9 is 1114.03 Å^3, or an intermetallic → oxysalt volume increase of +24.8%. The average *linear* increase is

$$\Delta = [(11.398 - 10.367)/11.398] \times 100 = +9.0\%,$$

a value indeed larger than the corresponding value for forsterite olivine. The kornerupine value is slightly larger than that for the ($\frac{1}{2}Al_2O_3$–Al) pair, and the less abundant Mg and Si nearly offset each other.

Table 13. Number of bonds of various types in olivine and kornerupine

Code	Olivine	Kornerupine*
1	0	0
2	12	9.6
3	8	8.0
3a	8	4.8
4	24	25.6
4a	32	25.6
4b	4	0
4c	8	0
5	0	2.4
5a	0	12.8
5b	0	2.4
Total	96	91.2

* Considering one-fifth the kornerupine cell (the unit for comparison).

Conclusions

The individual thermal-vibration parameters for the refined kornerupine in this study and two other refined kornerupines in the literature were compared. Comparison was based on the *difference*, $\Delta(\%)$, between kornerupine in this study (from Mautia Hill) and the other kornerupines.

For thermal vibrations, $\Delta(\%) = [(B - A)/A] \times 100$ where B = other kornerupines and A = the kornerupine in this study, from Mautia Hill. The individual U_{ii} ($i = 1$ to 3) values were compared. This gave an estimate of differences in which the values for other kornerupines are relatively less or greater than those for the Mautia Hill kornerupine of this study. The mean $|\Delta|$ of U_{ii} gave 25% for 8 unique cations and 17% for 10 unique anions. The mean $|\Delta|$ of B_{eq} gave 20% for the 8 cations and 3% for the 10 anions. In addition to reflecting the substitutional disorder of different kinds in kornerupine cation sites, these averages suggest that thermal parameters have some physical reality, at least for adequately refined structures. Note that comparison between anion sites shows remarkable concord.

A novel interpretation of the complex kornerupine crystal structure suggests that its cations are approximately isopunctal to the metals for intermetallic Ni_2In. Six larger cations [X, M(1)–M(5)] match up with three Ni(1) and three Ni(2), and three tetrahedral cations [T(1)–T(3)] match up with three of the more electronegative In. The mean difference using the kornerupine cell is 0.26 Å. A similar calculation for olivine with two octahedral and one tetrahedral cation gives a mean difference using the olivine cell of 0.46 Å. It was deemed sensible to inquire about the placement of the electronegative oxide anions in the collection of cations. In the sequence $[P_4\psi_4]$ (ψ = electron lone pair) → $[P_4O_6\psi_4]$ → $[P_4O_{10}]$, midpoints of P–P tetrahedral edges were taken and compared with the oxide centroids. The difference between the two is ~0.8 Å and suggests that oxygen fills its octet by exploiting P–P bond pairs. The same was done for kornerupine and olivine, respectively, both compared with Ni_2In. Differences between the ten oxide centroids and the cations corresponding to three Ni–Ni, one In–In, and six Ni–In midpoints led to a mean of 0.68 Å for kornerupine. In olivine, a similar calculation involving three Ni–In midpoints gave a mean of 0.93 Å. These calculations are summarized in Table 10.

Finally, it was asked how the structures distort when oxides are inserted into corresponding intermetallics. Again the *difference*, $\Delta(\%) = [(A - B)/A] \times 100$, where A = component oxide and B = intermetallic, was calculated for major components in kornerupine and olivine. These pairs were arranged according to valence electrons on the metal. It was observed that for M → MO, the linear change is *negative*—i.e., metal oxides have smaller volumes than isopunctal metals for those metals with *s* bonds only—but *positive* if *s* and *p* bonds are involved. This substantiates Pauling's (1960) statement that *p* bond strengths are greater than *s* bond strengths. An additivity relation was invoked to calculate the linear difference between $Mg_{0.677}Al_{1.310}Si_{0.679}O_{4.00}$ (modified kornerupine) and its "intermetallic" counterpart. Here, $\Delta = +9.0\%$, a value slightly larger than the ($\frac{1}{2}Al_2O_3$–Al) pair. For olivine, a similar calculation gave $\Delta = +3.2\%$, reflecting the predominance of *s* bonds for Mg metal in Mg_2Si.

These calculations suggest that relations between complex oxysalts and their corresponding intermetallics may place severe limitations on which oxysalt structures can exist and thus may further our understanding of their structure genealogy by exploiting corresponding isopunctal or near-isopunctal intermetallic phases.

Since the pioneering paper of O'Keeffe and Hyde (1985), a lot of work remains to be done. Their study involved mostly relatively simple systems, and questions of dilation due to oxygen insertion remain in abundance. Although tables of radii for oxides and fluorides are well established, analogous tables for nitrides, phosphides, arsenides, stibnides, carbides, silicides, stannides, etc., do not exist. Anisotropic distortion as a consequence of insertion of some electronegative atoms has barely been examined at all. In fact, no quantitative rules have appeared regarding cell expansion when progressing from intermetallic to oxysalt. Finally, it is not clear how great distortions can be for intermetallics, and how they should be described. A great many new intermetallic-oxysalt relationships have evolved in the laboratory of the senior author, most involving oxysalt structures of considerable complexity such as β-Cu_3As—painite and fluoborite; CoSn—crandallite, mitridatite; Ni_2In—glaserite, fillowite, α-$Ca_3(PO_4)_2$, stanfieldite, graftonite, dickinsonite, triploidite, triplite; $Fe_{12}Zr_2P_7$—dumortierite; Co_2Si—warwickite. But it is felt that before a great rush is made in search of structural gold, criteria for relatedness, adjacency, contiguity, and similarity must be evolved first.

Acknowledgments

Edward S. Grew, through his persistent prodding and insistence that yet more kornerupine chemical crystallography was necessary, perhaps more than anyone is responsible for the completion of this project. The senior author and Professor Grew share a common love for "-ine" minerals: kornerupine, "prismatine" and sapphirine, even ashcroftine and steenstrupine!

P.B.M. acknowledges the National Science Foundation Grant EAR 87-07382, and P.K.S. thanks the Tennessee computation facilities at the Tennessee Earthquake Information Center for use of their VAX computer.

References cited

Baur, W.H. (1970) Bond length variation and distorted coordination polyhedra in inorganic crystals. Transactions of the American Crystallographic Association, 6, 129–155.

Birle, J.D., Gibbs, G.V., Moore, P.B., and Smith, J.V. (1968) Crystal structures of natural olivines. American Mineralogist, 53, 807–824.

Cruickshank, D.W.J. (1964) Refinements of structures containing bonds between Si, P, S, or Cl and O or N. V. $\cdot P_4O_{10}$. Acta Crystallographica, 17, 677–679.

de Decker, H.C.J., and MacGillavry, C.H. (1941) Die Krystallstruktur des flüchtigen metastabilen Phosphorpentoxyds. Recueil des Travaux Chimiques des Pays-Bas, 60, 153–175.

Donnay, J.D.H., and Donnay, G., Eds. (1963) Crystal data (2nd edition).

American Crystallographic Association Monograph 5. William and Heintz Map Corporation, Washington, D.C.

Finger, L.W., and Hazen, R.M. (1980) Refinement of the crystal structure of an iron-rich kornerupine. Carnegie Institution of Washington Year Book 80, 370–373.

Hampson, G.C., and Stosick, A.J. (1938) The molecular structure of arsenious oxide, As_4O_6, phosphorus trioxide, P_4O_6, phosphorus pentoxide, P_4O_{10}, and hexamethylenetetramine, $(CH_2)_6N_4$, by electron diffraction. Journal of the American Chemical Society, 60, 1814–1822.

Ibers, J.A., and Hamilton, W.C., Eds. (1974) International tables for X-ray crystallography, Vol. 4, p. 99–100. Kynoch Press, Birmingham, England.

Laves, F., and Wallbaum, H.J. (1942) Über einige neue Vertreter des NiAs-Typs und ihre kristallchemische Bedeutung. Zeitschrift für Angewandte Mineralogie, 4, 17–46.

Lewis, G.N. (1916) The atom and the molecule. Journal of the American Chemical Society, 38, 762–785.

Maxwell, L.R., Hendricks, S.B., and Mosley, V.M. (1935) Electron diffraction by gases. Journal of Chemical Physics, 3, 699–709.

McKie, D. (1965) The magnesium aluminium borosilicates: Kornerupine and grandidierite. Mineralogical Magazine, 34, 336–357.

Moore, P.B., and Araki, T. (1979) Kornerupine: A detailed crystal-chemical study. Neues Jahrbuch für Mineralogie Abhandlungen, 134, 317–336.

Moore, P.B., and Bennett, J.M. (1968) Kornerupine: Its crystal structure. Science, 159, 524–526.

O'Keeffe, M., and Hyde, B.G. (1985) An alternative approach to non-molecular crystal structures, with emphasis on the arrangements of cations. Structure and Bonding, 61, 77–144.

Pauling, L. (1960) The nature of the chemical bond (3rd edition), p. 108–111. Cornell University Press, Ithaca, New York.

Shannon, R.D., and Prewitt, C.T. (1969) Effective ionic radii in oxides and fluorides. Acta Crystallographica, B25, 925–946.

Villars, P., and Calvert, L.D. (1985) Pearson's handbook of crystallographic data for intermetallic phases, vols. 1–3, 3258 p. American Society for Metals, Metals Park, Ohio.

Wells, A.F. (1975) Structural inorganic chemistry (4th edition), p. 673–686. Clarendon Press, Oxford, England.

Zachariasen, W.H. (1968) Experimental tests of the general formula for the integrated intensity of a real crystal. Acta Crystallographica, A24, 212–216.

Manuscript received September 14, 1987
Manuscript accepted January 19, 1989